Research papers

The influence of non-uniform blockages on transient wave behavior and blockage detection in pressurized water pipelines

H.F. Duan[a,*], P.J. Lee[b], T.C. Che[a], M.S. Ghidaoui[c], B.W. Karney[d], A.A. Kolyshkin[e]

[a] Department of Civil and Environmental Engineering, The Hong Kong Polytechnic University, Hung Hom, Kowloon, Hong Kong, China
[b] Department of Civil and Natural Resources Engineering, The University of Canterbury, Private Bag 4800, Christchurch, New Zealand
[c] Department of Civil and Environmental Engineering, The Hong Kong University of Science and Technology, Clear Water Bay, Kowloon, Hong Kong, China
[d] Department of Civil Engineering, University of Toronto, Toronto, ON M5 S 1A4, Canada
[e] Department of Engineering Mathematics, Riga Technical University, Riga LV1048, Latvia

ARTICLE INFO

ABSTRACT

Blockages in piping systems are formed from potentially complex combinations of bio-film build up, corrosion by-products, and sediment deposition. Transient-based methods seek to detect blockages by analyzing the evolution of small amplitude pressure waves. In theory, such methods can be efficient, nearly non-intrusive and economical but, thus far, studies have only considered symmetrical blockages, uniform in both the radial and longitudinal directions. Laboratory experiments are described here that involve pipe blockages with various levels of irregularity and severity; the way the transient response is affected by a non-uniform blockage is investigated. The differences between uniform and non-uniform blockages are quantified in terms of the rate that wave envelopes attenuate and the degree that phases are shifted. Two different methods for modeling these impacts are compared, namely through an increase in pipe roughness and through a wave scattering model. Wave scattering is shown to play a dominant role in explaining both wave envelope attenuation and phase shift. The accuracy of existing transient-based methods of blockage detection in the frequency domain is also examined, and is found that the predictions of rough blockage locations and sizes by current method are in good agreement with data, with relatively larger discrepancies for rough blockage lengths.

1. Introduction

Constrictions in pipe cross-sectional area, in the form of partial blockages, can form naturally on pipe walls and can gain significant lengths in water pipelines (see Fig. 1). In water supply pipes, drainage pipes, crude oil pipes, and arterial line systems, many factors can lead to the generation of these blockages including bio-film build up, corrosion, and sediment deposition. These blockages can cause additional energy loss and thus either an increase in pumping costs or a reduction in performance. Under unsteady flows, blockages often modify the pressure response and affect the effectiveness of surge mitigation devices. Duan et al. (2011a) show that transient wave scattering in pipes due to irregular and non-uniform blockages may cause attenuation of the wave envelope and shifts in the wave phase. These shifts are caused by a temporal and spatial redistribution of energy, not a dissipation of energy.

The study of transient pressure responses and its deviation from the expected response provide a means of condition diagnosis and numerous transient-based methods have been developed for detecting leaks and blockages in pipeline systems (Brunone, 1999; Ferrante and Brunone, 2003; Wang et al., 2002, 2005; Covas et al., 2005; Mohapatra et al., 2006; Lee et al., 2006, 2008, 2013; Sattar et al., 2008; Stephens, 2008; Meniconi et al., 2011, 2013; Duan et al., 2011b, 2012, 2013, 2014). The methods typically inject a customized pressure wave into the pipeline and fault properties are determined from the temporal or spectral analyses of the measured responses at different locations (Lee et al., 2013). In these applications, since the detailed geometry of the pipe blockages is initially unknown, pipe blockages are approximated either as uniform constrictions in the radial and longitudinal direction or inner wall roughness represented by different friction factors (Brunone et al., 2008; Stephens, 2008; Ebacher et al., 2011; Duan et al., 2012, 2013, 2014; Meniconi et al., 2011, 2012, 2013). These simplifications neglect the complex interaction of blockage irregularities and non-uniformities, and thus false adjustments of friction factors, wave speeds, and material properties often substitute for real pipe states (McInnis and Karney, 1995; Ebacher et al., 2011; Stephens et al., 2013; Duan et al., 2010a, 2013). It is noted that these adjustments are non-physically based and their necessity highlights the fact key behaviors
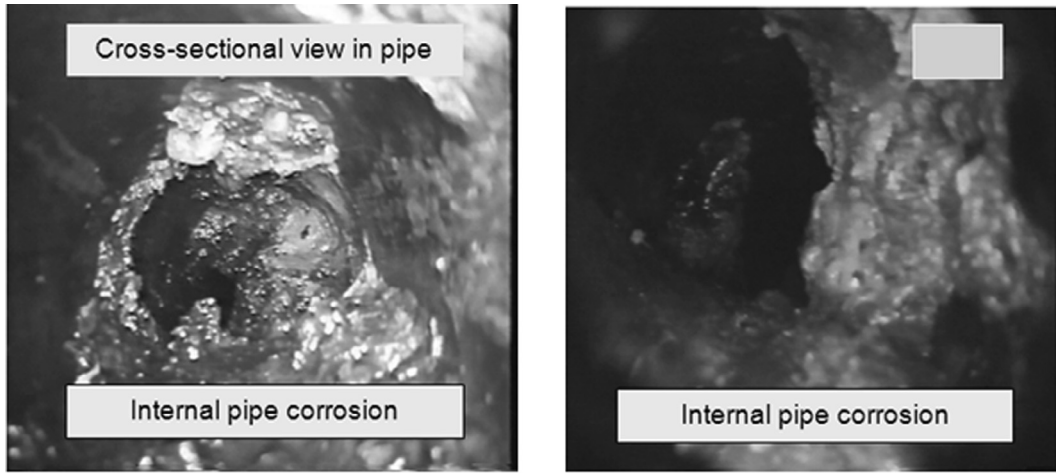
Fig. 1. Variation of pipe inner diameters observed in an aged urban water supply main. adapted from Stephens (2008)

are not modelled accurately within these models.

Despite numerous published works on blockage detection, experimental studies have not yet tested blockages of irregular geometries and little is known regarding the way non-uniform blockages alter the transient response. Can non-uniform blockages be usefully represented as uniform pipe constrictions or pipes of large roughness? Are wave scattering effects due to the blockage irregularities important? In this paper, numerical and experimental tests are conducted for blockages of different geometries to achieve three specific ends: (1) to identify the changes that blockage non-uniformity impose on the transient response; (2) to compare the accuracy of different modeling approaches for the non-uniform blockage; and (3) to examine the accuracy of current blockage detection method when applied to a non-uniform blockage. The aim of the study is to improve the modeling and detection approaches for the non-uniform blockages.

2. Models and methods

2.1. Numerical model and simulation scheme

In this study, the 1D continuity and momentum equations of unsteady pipe flows are used for the numerical simulations, with following expressions (Wylie et al., 1993; Ghidaoui et al., 2005; Duan et al., 2011a),

$$\frac{\partial(\rho A)}{\partial t} + \frac{\partial(\rho Q)}{\partial x} = 0, \tag{1}$$

$$\frac{\partial(\rho Q)}{\partial t} + A\frac{\partial P}{\partial x} + \pi D\tau_w = 0, \tag{2}$$

where ρ = fluid density; $A = A(x)$ = pipe cross-sectional area; $D = D(x)$ = pipe internal diameter; $Q = Q(x, t)$ = pipe discharge; $P = P(x, t)$ = pressure; x = spatial coordinate; and t = temporal coordinate; $\tau_w = \tau_w(x, t)$ = wall shear stress. To represent the damping effect of rough pipe blockages, the Colebrook–White equation based Darcy friction factor (Wylie et al., 1993) and the unsteady friction model for rough pipe flows in Vardy and Brown (2004) are used to describe the wall shear stress as follows:

$$\tau_w = \frac{\rho f|Q|Q}{8A^2} + \frac{4\nu\rho}{AD}\int_0^t \frac{\alpha e^{-\beta(t-t')}}{\sqrt{\pi(t-t')}}\frac{\partial Q}{\partial t}dt' \tag{3}$$

where f = friction factor based on the Colebrook–White equation; ν = kinematic viscosity of fluid; t' = a dummy variable representing the instantaneous time in the time history; α, β = coefficient, and

(i) for turbulent smooth pipe flows,

$$\alpha = \frac{D}{4\sqrt{\nu}} \quad \text{and} \quad \beta = \frac{0.54\nu}{D^2}\mathbf{Re}_0^{\log(14.3/\mathbf{Re}_0^{0.05})}, \tag{4a}$$

(i) for turbulent rough pipe flows,

$$\alpha = 0.00913\left(\frac{\varepsilon}{D}\right)^{0.39}\sqrt{\frac{D^2}{\nu}\mathbf{Re}_0} \quad \text{and} \quad \beta = 1.408\left(\frac{\varepsilon}{D}\right)^{0.41}\frac{\nu}{D^2}\mathbf{Re}_0, \tag{4b}$$

in which, ε = pipe wall roughness; $\mathbf{Re}_0$ = initial Reynolds number.

To obtain the numerical results (e.g., pressure head), the method of characteristics (MOC) with a 2nd-order discretization accuracy scheme, which has been well developed in previous studies of the authors (e.g., Duan, 2011c; Ghidaoui et al., 2005), is used to solve above models for the experimental pipeline system established later in this paper.

2.2. Theoretical model of wave scattering by rough blockage

In addition to friction damping, the non-uniform blockage scatters waves. The wave scattering attenuates the main signal as shown in Duan et al. (2011a) in which an analytical relationship between the incident waves and the non-uniformity of the blockage is derived. Duan et al. (2011a) show that the wave scattering causes the energy to be spread over multiple waves and is distinct from frictional dissipation effects. The wave envelope was found to be reasonably modelled through an exponential decay function:

$$B = B_0 e^{-\lambda x} = B_0 e^{-a\lambda t}, \tag{5}$$

where $B = B(x)$ = amplitude of wave envelope with distance along the pipeline or with the equivalent time $t = x/a$ with a = wave speed; B_0 = amplitude of the incident wave; $\lambda = \lambda_r - i\lambda_i$, i = imaginary unit, and λ_r and λ_i = wave damping factor and wave phase change (frequency shift) factor, respectively, such that:

$$\lambda_r = \frac{\alpha k^2 \delta_A^2}{\alpha^2 + 4k^2}, \quad \text{and} \quad \lambda_i = \frac{k\alpha^2 \delta_A^2}{2(\alpha^2 + 4k^2)}, \tag{6}$$

in which δ_A = coefficient of variation (COV) of the pipe cross-sectional area in the spatial domain which quantifies the irregularity of the blockage severity and $\delta_A = \sigma_A/\mu_A$ with σ_A and μ_A being the standard deviation and mean values of the pipe area; k = incident wave number and $k = \omega/a$, with ω = wave frequency; α = spatial correlation coefficient of the blockage and $\alpha \sim 1/L_c$ with L_c = correlation length which describes the spatial variability of the blockage. The neglect of pipe friction effect in these expressions allows the relative importance of wave scattering to be compared to pipe friction later in this study. The

wave speed (a) in above result is a lumped parameter that represents the properties of pipe-wall material and internal fluid (water), including the elasticity and thickness of pipe-wall, and the density and bulk modulus of fluid (Duan et al., 2010a). This lumped parameter will be calibrated in advance for the test pipeline system in this study based on the preliminary transient tests (Wylie et al., 1993). It is also noted that the derivation of this wave scattering result in Duan et al. (2011a) has not yet included complex boundary conditions such as water tank and valve. Therefore, it is impossible to apply this derived result for complete blockage detection, but it is useful to conduct a forward inspection and comparison with results from other methods in terms of the influence of rough blockages on the envelop attenuation and frequency shift.

2.3. Laboratory experimental setup and test cases

Experiments at the University of Canterbury, New Zealand allowed the study of the effects non-uniform blockages and a comparison of different approaches for approximating the physics behind the blockage-wave interaction. The testing system consists of an upstream pressurized water tank with a constant pressure head of 38.2 m, a 41.53 m length of pipeline, and a downstream discharge tank, as shown in Fig. 2. All joints within the system are custom-made flange connections with minimum intrusion into the flow to avoid internal distortions. The two inline valves located at the upstream and downstream ends are used to control the initial flow (Q_0), while the side-discharge vale at downstream end (adjacent to the downstream inline valve) is used for transient wave generation. The side discharge valve is initially open under steady state conditions and then slammed shut within a time of about 6 ms to generate the transient wave. For blockage testing, the pipeline is divided into three sections, where the initial and last sections are uniform and steel pipes with a diameter of $D_0 = 73.2$ mm, while the middle section is used to insert different blockage sections.

The parameters and settings for the test systems are shown in Table 1, two types of non-uniform blockages are tested in this study: one is made from irregular rock aggregates (test No.3); and the other is made from rough coconut coir (test No. 4). For comparison, tests for a pipe system without blockage and a pipe with a uniform blockage (tests No. 1 and No. 2) are also conducted.

Transient waves are generated downstream by the fast closure of the side-discharge valve (see Fig. 2a) from an initially fully open state at around 0.011 s. For each test, the transient pressure data are collected at the side discharge valve in Fig. 2(a) by the pressure transducer with a sampling frequency of 20 kHz. The range of initial Reynolds number

(Re_0) along the pipeline (with sections different diameters) for the tests is listed in Table 1. The flow diameter of the non-uniform blockage section (D_b) shown in Table 1 is the average pipe flow diameter along the blockage section, and the coefficient of variation (COV) of the blockage cross-sectional area (δ_A) is estimated from the maximum and minimum values for the area (A_{max} and A_{min}) by Tung et al. (2006) as:

$$\delta_A = \frac{A_{max} - A_{min}}{2\sqrt{3} A_b} \quad \text{with} \quad A_b = \frac{\pi}{4} D_b^2 \tag{7}$$

For convenient comparison and systematic analysis, extensive numerical simulations are conducted later in this study for this experimental pipeline system in Fig. 2 under different pipe material and flow conditions. To this end, the roughness or equivalent friction factor (f) in the friction model of Eq. (3) for different test pipe sections above have been calibrated in advance by the steady-state flow condition (Potter et al., 2012). The calibrated results show that, for the test cases of interest in this study, $f = 0.022$ for uniform and steel pipe sections, $f = 0.056$ for the blockage section of rock aggregate, and $f = 0.052$ for that of rough coir. It is also noted that the numerical simulations by Eqs. (1) and (2) will not simulate directly the pipe materials and pipe-wall deformation effects in the model. Instead, a lumped parameter, wave speed (a), has been developed in the waterhammer literature and commonly used to represent these complex effects under transient flow conditions (Wylie et al., 1993; Ghidaoui et al., 2005):

$$a = \sqrt{\frac{K}{\rho\left(1 + C\frac{KD}{Ee}\right)}}, \tag{8}$$

where K = bulk modulus of fluid elasticity; E = Young's modulus of pipe elasticity; e = pipe thickness; and C = pipe constraint coefficient. As a result, the wave speed defined in Eq. (8) represents combined effects of the fluid compressibility and elastic pipe-wall flexibility on the mass storage due to pressure change in the pipeline. The wave speed for each experimental test in this study is calibrated in advance for extensive numerical simulations later in this study (Duan et al., 2013), and the average results are shown in Table 1.

3. Results and discussion

3.1. Influence of non-uniform blockages on the transient responses

The transient responses for all scenarios are plotted in Fig.3(a). The vertical coordinate is the pressure perturbation from steady state (ΔP_t) normalized by the maximum value in the transient trace (ΔP_{max}). Fig. 3(a) clearly shows that blockages cause noticeable changes in the
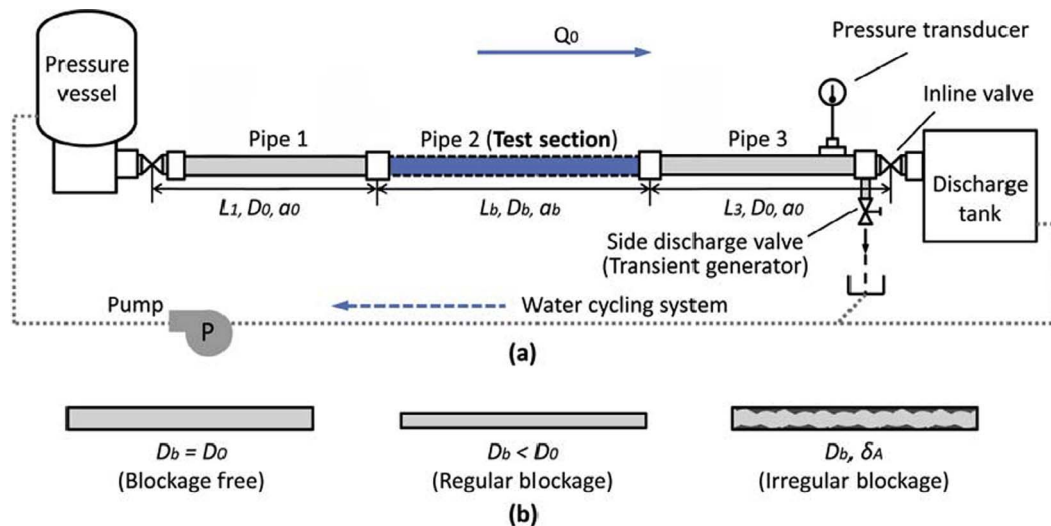

Fig. 2. (a) Sketch of experimental test system; (b) inserted sections for different tests.

Table 1
Settings for experimental test systems.

Test No. and blockage type	Uniform pipe sections				Blockage section				$\mathbf{Re_0}$ ($\times 10^3$)
	L_1 (m)	L_3 (m)	D_1 ($=D_3$) (mm)	a_1 ($=a_3$) (m/s)	L_b (m)	D_b (mm)	a_b (m/s)	δ_A	
1: Blockage-free	15.53	20.41	73.2	1180	5.59	73.2	–	–	2.7–67.5
2: Uniform blockage	15.53	20.41	73.2		5.59	22.2	1320	–	
3: Rough aggregate blockage	15.53	20.41	73.2		5.59	59.3	1050	0.096	
4: Rough coir blockage	15.58	20.41	73.2		5.54	59.6	1010	0.127	

Fig. 4. Time-domain result comparison of transient envelopes by different numerical treatments of rough blockages and experimental measurements.
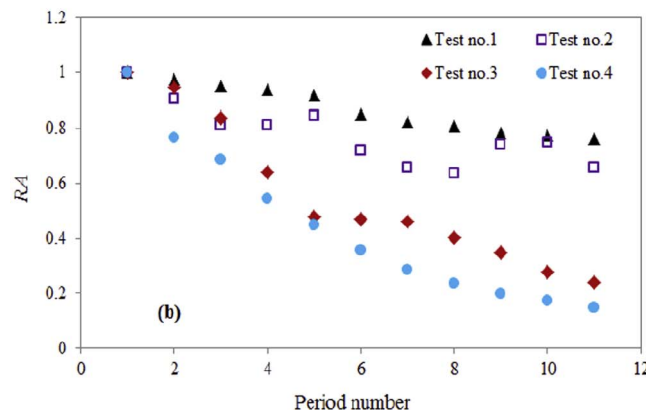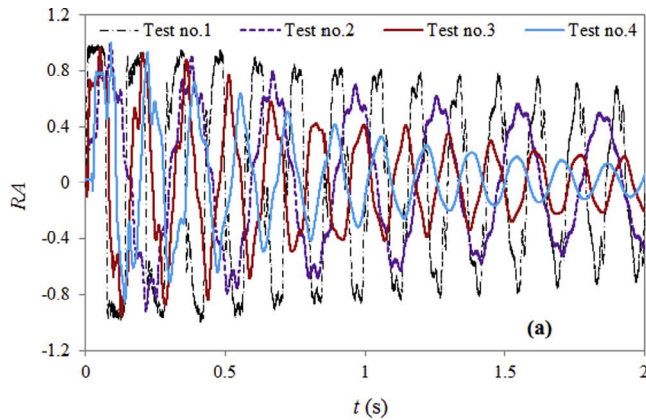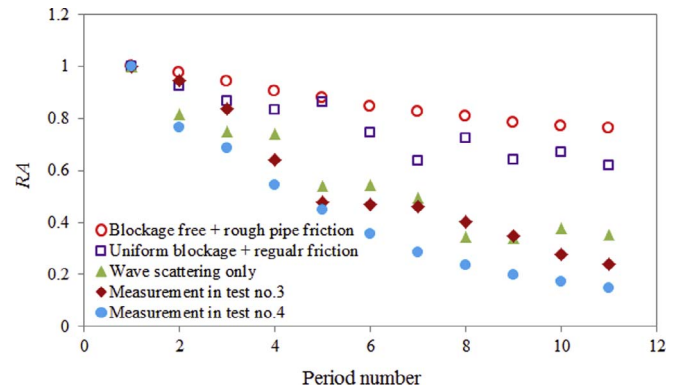

Fig. 3. (a) Partial time-domain results of measured transient waves for three test cases (0–2 s); (b) Extracted envelopes for experimental tests (Test No. 1 for blockage-free case; Test No. 2 for uniform blockage case; Test No. 3 for rough aggregate blockage case; Test No. 4 for rough coir blockage case).

rate of signal attenuation and period of the signal.

For illustration, the extracted wave envelope results for the four scenarios are shown in Fig. 3(b), a plot that shows that the blockage irregularity noticeably alters the transient attenuation. The dimensionless wave amplitude in the non-uniform blockages (tests 3 and 4) decreased to half of that in the uniform and blockage free cases (test 1 and 2) after just 10 cycles even though the blockage severity of the uniform blockage case is much larger than that of the irregular case (Table 1); this is a consequence of the difficulty in constructing a severe constriction using irregular and granular material. Despite the lower constriction severity, the non-uniform blockages result in greater attenuation of the transient signal strongly suggesting that the transient wave amplitude attenuation is strongly influenced by the blockage irregularity.

3.2. Effects of rough blockages on transient wave attenuation

The relative effects of friction and wave scattering in the presence of

rough blockages is next numerically explored. The rough blockage section is modelled using three approaches. First, the blockage is modelled using rough pipe friction model (Eqs. (3) and (4b)), but neglecting any diameter effects. The second approach replaces the rough blockage by an equivalent uniform blockage whose diameter is equal to the average diameter of the rough blockage and whose friction is governed by the smooth pipe model (Eqs. (3) and (4a)). The third approach treats the blockage as a frictionless wave scatterer using the numerical scheme in Duan et al. (2011a), where 40 random pipe reaches are used to represent the rough blockage section. The results of the three approaches are plotted in Fig. 4 together with the experimental data for case No. 3. The results of the other cases display similar trends and are not shown here.

The results in Fig. 4 clearly indicate: (i) the inadequacy of the first approach (i.e., the rough pipe friction model only provides poor representation of the wave envelope of the rough pipe blockages); (ii) the inadequacy of the second approach (i.e., the common approach of using a uniform constriction together with smooth friction law to represent a rough blockage provides inaccurate representation of the wave envelope); and (iii) the relative superiority of the third approach since treating a rough blockage as a random scatterer provides a wave envelope comparable to measurements. Consequently, the analysis of wave scattering becomes invaluable for transient modeling and analysis of rough blockages.

Furthermore, the results of transient wave envelope attenuation by the wave scattering and rough friction effects are examined in the frequency domain. The measured and numerical wave signals for the irregular blockage case in Fig. 3 are converted into the frequency domain and compared. In the frequency domain, the numerical wave scattering effect can be obtained using two methods: one is converted directly from the time-domain result in Fig. 4, and the other is calculated based on Eqs. (5) and (6). Duan et al. (2011a) has shown that both methods provide similar results and only the analytical calculated result is used here for comparison. Correspondingly, the numerical frequency-domain results of the wave scattering and friction effects for both the rough and regular blockages and the experimental measurements for the two different rough blockage cases are shown in Fig. 5 which visually confirms that the wave scattering effect of the rough blockage
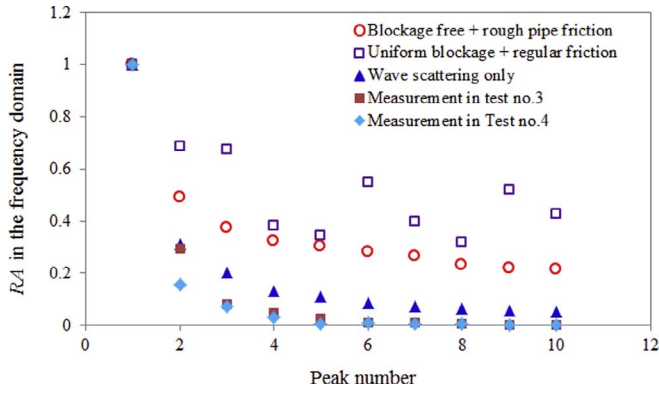
Fig. 5. Frequency-domain result comparison of transient envelopes by different numerical treatments of rough blockages and experimental measurements.

dominates the frictional effect.

3.3. Effects of rough blockages on transient wave phase change

In addition to wave attenuation, extended blockages often cause shifts in wave phase (frequency shift), an important effect for extended blockage detection (Duan et al., 2012, 2013, 2014; Lee et al., 2013). To this end, numerical tests were conducted for the rough blockage cases (tests No. 3 and No. 4). Again, the rough blockage section is treated in two ways: as a pipeline with large pipe roughness heights and as a constricted uniform pipe.

Fourier transforms of the time-domain results allow the extraction of the resonant peak frequencies as are shown in Fig. 6(a) and (b) for test cases No. 3 and No. 4 respectively. The vertical coordinates show the relative frequency shift from the original blockage-free pipeline case (test No. 1), which is defined by the difference of resonant frequency
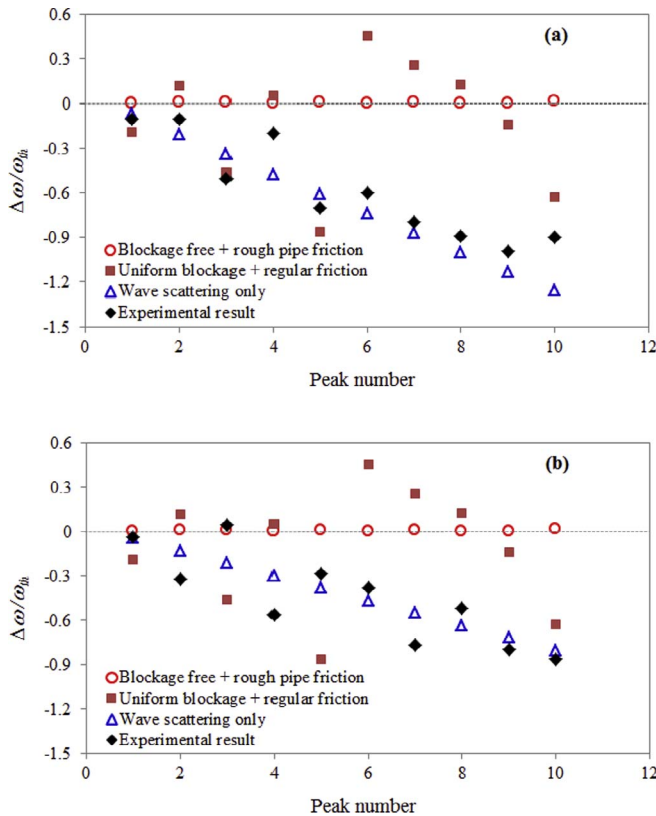

Fig. 6. Results of relative frequency shift to blockage-free pipeline by rough blockage for: (a) test No. 3; (b) test No. 4.

between the blockage-free and blockage situations ($\Delta\omega$) and normalized by the theoretical frequency of the system (ω_{th}). The experimental results for rough blockage tests No. 3 and No. 4 are also plotted in the same figure for comparison. Fig. 6 clearly shows the significant discrepancy between the two different approximations of the rough blockage. Treating the blockage as an increased pipe roughness clearly has little impact on the resonant frequency shifts, a result that is consistent with similar findings in Duan et al. (2010b) and Lee et al. (2013). However, treating the rough blockage as a constricted uniform pipe section shows significant frequency shifts.

However, Fig. 6 shows that neither of these first two approximations closely reproduces the observed frequency shifts (phase changes). The irregularity and non-uniformity of rough blockage causes frequency shifts in the transient responses that cannot be replicated by approximating the rough blockage as a rough section of pipe or as a constricted section of pipe. In contrast, the results of wave scattering based on Eq. (5) are calculated and plotted in Fig. 6(a) and (b) for the two test cases, which show a more accurate representation in both trends and amplitudes for the influence of rough blockage on the frequency shifts. Clearly, these comparative results demonstrate the importance of the wave scattering effect in the frequency response of pipelines with rough extended blockages. This result can potentially affect the applicability of frequency-domain transient-based methods developed in the literature (e.g., Duan et al., 2012; Lee et al., 2013) which was based on the approximation of the blockage as a constricted uniform pipe.

3.4. Influence of rough blockages to existing blockage detection method

With this experimental confirmation of the importance of wave scattering effect in the dynamics of rough extended blockages, it is necessary to examine the applicability of current transient-based blockage detection methods that were developed without wave scattering in mind. In this study, the transient-based frequency domain method for blockage detection developed in Duan et al. (2012) is taken as an example, which is described in the following section.

3.4.1. Transient-based frequency domain method of blockage detection

The governing equations (1) and (2) can be converted into the frequency domain equivalents in the form of transfer matrices, giving the resonance condition for a pipeline systems with a single extended blockage as (Duan et al., 2012),

$$\begin{pmatrix} (Y_u + Y_b)(Y_b + Y_d)\cos[(\lambda_u + \lambda_b + \lambda_d)\omega_{rf}] \\ + (Y_u - Y_b)(-Y_b - Y_d)\cos[(\lambda_u - \lambda_b - \lambda_d)\omega_{rf}] \\ - (Y_u + Y_b)(Y_b - Y_d)\cos[(\lambda_u + \lambda_b - \lambda_d)\omega_{rf}] \\ - (Y_u - Y_b)(-Y_b + Y_d)\cos[(\lambda_u - \lambda_b + \lambda_d)\omega_{rf}] \end{pmatrix} = 0,$$

(9)

where, $\omega_{rf} = \omega_{rf}(n)$ is the resonant frequency for the nth resonant peak; $\lambda = C_R l/a$ is the wave propagation operator; l is the pipe section length; $C_R = \sqrt{1 - igAR/\omega}$ is the friction influence coefficient; $Y = -C_R a/gA$ is the transient impedance coefficient; $R = fQ/gDA^2$ is the friction damping factor; g is the gravitational acceleration; and subscripts "u, b, d" represent the pipe sections upstream of the blockage, the pipe section with the blockage and the pipe section downstream of the blockage respectively. For a single blockage, $Y_u = Y_d = Y_0$ in Eq. (9) with subscript "0" representing the quantity of original blockage-free (intact) pipeline. The total friction effect (steady and unsteady components) contained in the damping factor R is determined by the formulations in Eq. (3). In the application of blockage detection, the resonant frequencies $\omega_{rf}(n)$ (with $n = 1, 2, 3...$) are measured or simulated from the testing pipe system, and then substituted into Eq. (9) to inversely determine the blockage properties (size, length and location). The application procedures are detailed in Duan et al. (2012).

3.4.2. Blockage detection results and analysis

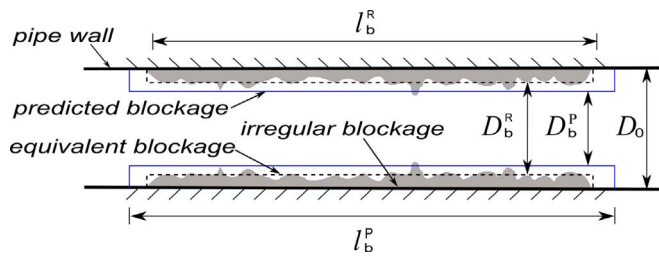In the development of this method in Eq. (9), the extended blockage

Fig. 7. Schematic of irregular blockage detection in the pipeline.

is approximated as a regular and symmetric constriction of pipe area; and for this reason, the method cannot provide the detailed spatial distribution of an irregular blockage. Instead, in this study, this method will be used to estimate the equivalent (averaged) extended blockage properties (D_b and l_b) as illustrated in Fig. 7. By applying the genetic algorithm (GA) based optimization procedure (Duan and Lee, 2016) where the first 10 measured responses (i.e., resonant frequencies) are matched to Eq. (9), the predicted results for the three blockages cases (cases No. 2 to No. 4 in Table 1) are listed in Table 2.

To evaluate the accuracy of the detection results, the prediction error of each blockage parameter is defined as:

$$\gamma(\%) = \frac{Z^P - Z^R}{Z^R} \times 100, \tag{10}$$

where Z represents the each blockage parameter and $Z = D_b$, l_b, and l_d in this study, the superscripts "P" and "R" represent the predicted and real values respectively. The detection errors for the tests are calculated based on Eq. (10) and also given in Table 2.

The comparison of the results from Table 2 shows that the detection accuracy of all blockage parameters (l_d, l_b and D_b) for the regular blockage case (i.e., test No. 2) is much higher than that for the rough blockage cases (tests No. 3 and No. 4), which is reasonable given that this detection method was originally developed for the regular blockage case in Duan et al. (2012). Particularly, the maximum prediction error for the regular blockage case is less than 9%, which is consistent with the detection accuracy obtained in the former studies (Duan et al., 2012, 2013, 2014). However, the maximum error for the other two rough blockage cases in this study attain to 220% and 165% respectively (i.e., for the detection of blockage length), which are unacceptable for practical applications. From this point of view, this previously developed blockage detection method is poorly suited to accurately predict the details of rough blockages.

However, for all the regular and rough blockage cases, the detection accuracy for the blockage location is much higher than that for the blockage severities (size and length), with both errors within 6% which is acceptable for practical detection purpose. From this perspective, this transient-based blockage detection method is still practically useful, since identifying and locating potential blockages are first steps for the blockage detection process. Therefore, it is desirable to further develop and apply the transient-based method for the blockage detection and diagnosis of water pipelines, so that it could become an important and alternative tool for the maintenance and management of urban water pipeline systems. It is also noted that this result is obtained from the laboratory experiments and analysis for relatively small-scale pipeline

system adopted in this study.

Furthermore, the result comparison in Table 2 reveals that, for the rough blockage detection by the transient-based method, the estimated blockage constriction extent ($D_0 - D_b$) is more severe than the real situations (so that negative error with $\gamma < 0$), and the predicted blockage length (l_b) is much longer than the real case (as depicted in Fig. 7). In other words, the generated frequency shifts by irregular blockage are more severe than that by the equivalent (or averaged) regular extended blockage according to Eq. (8) (Duan et al., 2014), which again indicates that the frequency shift is highly affected by the irregularity of rough blockages for its wave scattering effect.

This application result provides further confirmation to the previous analysis in terms of the time domain and frequency domain results in this study as well as in many previous studies (Duan et al., 2013, 2014). Consequently, the application results here demonstrate again that the wave scattering of rough blockage irregularity plays an important role in the blockage detection accuracy of the current transient-based methods. It is necessary to investigate and include this effect in the development and application of transient-based blockage detection method in the future work. On this point, the analytical results and experimental tests of this study may provide a foundation for further improvement.

4. Conclusions and recommendations

The paper investigates, both experimentally and numerically, the transient wave behaviors under the conditions of two types of pipe blockages with different irregularities and their impacts on the transient wave analysis and utilization (blockage detection). Both wave scattering and rough friction effects from the rough blockages are examined for their influences to the transient wave attenuation and phase change respectively in comparison with the experimental measurement. The results indicate that the wave scattering effect from the rough blockages appears to play the dominant role, influencing both wave attenuation and phase change. Moreover, the influence of rough blockage irregularity to transient analysis and utilization is investigated by taking the existing transient-based frequency domain blockage detection method for illustration. The application results demonstrate that the limitations of current transient-based frequency domain detection method for predicting the blockage size (length and severity) for rough and irregular blockages because of the significant influences of the wave scattering from the rough blockages to the frequency shift that is currently ignored by this method. But the results also imply the applicability of this method for locating the potential rough blockages in practical pipeline systems. It is suggested for the necessity of considering and including wave scattering effect of rough blockages for the transient modeling and analysis in the future work.

This study clearly suggests further study is needed to accurately quantify the relative importance and contribution to transient wave attenuation and phase changes. Greater consideration of rough blockage seem warranted in order to better understand and predict wave scattering and rough friction effects from rough blockages. It is also necessary to mention that the results and analysis of this study are mainly based on the laboratory experimental system with relatively small scales and simple configuration conditions, and further investigations for practical and complex systems are worthwhile in the

Table 2
Detection results and accuracy of transient-based blockage detection.

Test No. and test case	Blockage size (mm)			Blockage length (m)			Blockage location (m)		
	D_b^R	D_b^P	(%)	l_b^R	l_b^P	(%)	l_3^R	l_3^P	(%)
2: Regular blockage	22.2	24.11	8.60	5.59	5.74	2.68	20.41	20.68	1.32
3: Rough aggregate blockage	59.3	52.08	−12.18	5.59	17.89	220	20.41	21.57	5.66
4: Rough coir blockage	59.6	52.73	−11.54	5.54	14.67	165	20.41	21.38	4.76

future work.

Acknowledgements

References

Brunone, B., 1999. Transient test-based technique for leak detection in outfall pipes. ASCE J. Water Resour. Plann. Manage. 125 (5), 302–306.

Brunone, B., Ferrante, M., Meniconi, S., 2008. Discussion of 'detection of partial blockage in single pipelines' by P.K. Mohapatra, M.H. Chaudhry, A.A. Kassem, and J. Moloo. ASCE J. Hydraulic Eng. 134 (6), 872–874.

Covas, D., Ramos, H., Almeida, A.B., 2005. Standing wave difference method for leak detection in pipeline systems. ASCE J. Hydraulic Eng. 131 (12), 1106–1116.

Duan, H.F., 2011c. Investigation of factors affecting transient pressure wave propagation and implications to transient based leak detection methods in pipeline systems (PhD Thesis), The Hong Kong University of Science and Technology, Hong Kong.

Duan, H.F., Lee, P.J., 2016. Transient-based frequency domain method for dead-end side branch detection in reservoir-pipeline-valve systems. ASCE J. Hydraulic Eng. 142 (2), 04015042.

Duan, H.F., Tung, Y.K., Ghidaoui, M.S., 2010a. Probabilistic analysis of transient design for water supply systems. ASCE J. Water Resour. Plann. Manage. 136 (6), 678–687.

Duan, H.F., Lee, P.J., Ghidaoui, M.S., Tung, Y.K., 2010b. Essential system response information for transient-based leak detection methods. IAHR J. Hydraulic Res. 48 (5), 650–657.

Duan, H.F., Lu, J.L., Kolyshkin, A.A., and Ghidaoui, M.S. (2011a). The effect of random inhomogeneities on wave propagation in pipes. In: Proceedings of the 34th IAHR Congress, June 26 – July 1, 2011, Brisbane Australia.

Duan, H.F., Lee, P.J., Ghidaoui, M.S., Tung, Y.K., 2011b. Leak detection in complex series pipelines by using system frequency response method. IAHR J. Hydraulic Res. 49 (2), 213–221.

Duan, H.F., Lee, P.J., Ghidaoui, M.S., Tung, Y.K., 2012. Extended blockage detection in pipelines by using the system frequency response analysis. ASCE J. Water Resour. Plann. Manage. 138 (1), 55–62.

Duan, H.F., Lee, P.J., Kashima, A., Lu, J.L., Ghidaoui, M.S., Tung, Y.K., 2013. Extended blockage detection in pipes using the frequency response method: analytical analysis and experimental verification. ASCE J. Hydraulic Eng. 139 (7), 763–771.

Duan, H.F., Lee, P.J., Ghidaoui, M.S., Tuck, J., 2014. Transient wave-blockage interaction and extended blockage detection in elastic water pipelines. J. Fluids Struct. 46 (2014), 2–16.

Ebacher, G., Besner, M., Lavoie, J., Jung, B., Karney, B., Prévost, M., 2011. Transient modeling of a full-scale distribution system: comparison with field data. ASCE J. Water Resour. Plann. Manage. 137 (2), 173–182.

Ferrante, M., Brunone, B., 2003. Pipe system diagnosis and leak detection by unsteady-state tests-1: harmonic analysis. Adv. Water Resour. 26 (1), 95–105.

Ghidaoui, M.S., Zhao, M., McInnis, D.A., Axworthy, D.H., 2005. A review of water-hammer theory and practice. ASME Appl. Mech. Rev. 58, 49–76.

Lee, P.J., Lambert, M.F., Simpson, A.R., Vítkovský, J.P., Liggett, J., 2006. Experimental verification of the frequency response method for pipeline leak detection. IAHR J. Hydraulic Res. 44 (5), 693–707.

Lee, P.J., Vítkovský, J.P., Lambert, M.F., Simpson, A.R., Liggett, J., 2008. Discrete blockage detection in pipelines using the frequency response diagram: numerical study. ASCE J. Hydraulic Eng. 134 (5), 658–663.

Lee, P.J., Duan, H.F., Ghidaoui, M.S., Karney, B.W., 2013. Frequency domain analysis of pipe fluid transient behaviors. IAHR J. Hydraulic Res. 51 (6), 609–622.

McInnis, D., Karney, B.W., 1995. Transients in distribution networks: field tests and demand models. ASCE J. Hydraulic Eng. 121 (3), 218–231.

Meniconi, S., Brunone, B., Ferrante, M., Massari, C., 2011. Potential of transient tests to diagnose real supply pipe systems: what can be done with a single extemporary test. ASCE J. Water Resour. Plann. Manage. 137 (2), 238–241.

Meniconi, S., Brunone, B., Ferrante, M., 2012. Water-hammer pressure waves interaction at cross-section changes in series in viscoelastic pipes. J. Fluids Struct. 33, 44–58.

Meniconi, S., Duan, H.F., Lee, P.J., Brunone, B., Ghidaoui, M.S., Ferrante, M., 2013. Experimental investigation of coupled frequency and time-domain transient test-based techniques for partial blockage detection in pipes. ASCE J. Hydraulic Eng. 139 (10), 1033–1040.

Mohapatra, P.K., Chaudhry, M.H., Kassem, A.A., Moloo, J., 2006. Detection of partial blockage in single pipelines. ASCE J. Hydraulic Eng. 132 (2), 200–206.

Potter, M.C., Wiggert, D.C., Ramadan, B.H., 2012. Mechanics of Fluids, fourth ed. Cengage Learning, Australia.

Sattar, A.M., Chaudhry, M.H., Kassem, A.A., 2008. Partial blockage detection in pipelines by frequency response method. ASCE J. Hydraulic Eng. 134 (1), 76–89.

Stephens, M.L., 2008. Transient response analysis for fault detection and pipeline wall condition assessment in field water transmission and distribution pipelines and networks (PhD Thesis). The University of Adelaide, South Australia.

Stephens, M., Lambert, M., Simpson, A., 2013. Determining the internal wall condition of a water pipeline in the field using an inverse transient. ASCE J. Hydraulic Eng. 139 (3), 310–324.

Tung, Y.K., Yen, B.C., Melching, C.S., 2006. Hydrosystems Engineering Reliability Assessment and Risk Analysis. McGraw-Hill Company, New York.

Vardy, A.E., Brown, J.M.B., 2004. Transinet turbulent friction in fully rough pipe flows. J. Sound Vib. 270 (1), 233–257.

Wang, X.J., Lambert, M.F., Simpson, A.R., Liggett, J.A., Vítkovský, J.P., 2002. Leak detection in pipeline systems using the damping of fluid transients. ASCE J. Hydraulic Eng. 128 (7), 697–711.

Wang, X.J., Lambert, M.F., Simpson, A.R., 2005. Detection and location of a partial blockage in a pipeline using damping of fluid transients. ASCE J. Water Resour. Plann. Manage. 131 (3), 244–249.

Wylie, E.B., Streeter, V.L., Suo, L., 1993. Fluid Transients in Systems. Prentice Hall, Englewood Cliffs, New Jersey.